DOI: https://doi.org/10.30546/19023.978-9952-610-87-1.2026.100.1144.
ISBN: 978-9952-610-87-1

EFFECT OF AOD REFINING ON INCLUSION MORPHOLOGY AND MICROSTRUCTURAL CLEANLINESS IN G17CRMO5-5 CAST STEEL

Öznur KILIÇ[1,2*], Prof. Dr. Kerem Altuğ GÜLER[1]

[1] Department of Metallurgical and Materials Engineering, Yildiz Technical University, Davutpasa Campus, Esenler, 34210 Istanbul, Turkey

[2]TÜBİTAK Marmara Research Center (MAM), Barış Neighborhood. Dr. Zeki Acar Street. No:1 P.K. 21 41470 Gebze / Kocaeli

ORCID ID: https://orcid.org/0009-0002-8524-7397

ABSTRACT

In this study, different melting and refining strategies were applied to G17CrMo5-5 cast steel in order to evaluate their influence on inclusion evolution and microstructural cleanliness. Two production routes were comparatively investigated. In the first route, the alloy was melted in an induction furnace, followed by sequential deoxidation using Fe–Si–Zr, Ca–Si, and aluminum. In the second route, induction melting was followed by Argon Oxygen Decarburization (AOD) refining, with deoxidation restricted to Ca–Si and aluminum additions. Comprehensive characterization was carried out, including metallographic analysis, detailed inclusion characterization, mechanical testing at ambient temperature and fracture surface examination by scanning electron microscopy. The results were evaluated comparatively with respect to the applied refining route and deoxidation practice. Particular attention was given to the relationship between inclusion chemistry, morphology, size distribution, and spatial arrangement within the matrix. The findings demonstrate that AOD refining promotes the transformation of complex, irregular oxide and oxysulfide inclusions into finer and more globular calcium-containing oxide phases, leading to a cleaner and more homogeneous microstructure. This inclusion modification reduces stress concentration sites and improves deformation continuity, which is reflected in the overall mechanical response of the alloy. The study highlights that the primary contribution of AOD processing in G17CrMo5-5 cast steel lies in effective inclusion control and microstructural refinement rather than direct compositional adjustment.

Keywords: G17CrMo5-5 cast steel; AOD refining; deoxidation practice; inclusion evolution

INTRODUCTION

Cr–Mo based cast steels are widely used in high-temperature and pressure applications due to their favorable strength, creep resistance, and thermal stability. Their mechanical performance depends not only on composition but also on microstructural cleanliness, inclusion morphology, and carbide distribution, particularly at elevated temperatures (Chaudhuri 1990, Aggen 2005). Low-alloy ferritic

DOI: https://doi.org/10.30546/19023.978-9952-610-87-1.2026.100.1144.
ISBN: 978-9952-610-87-1

steels (e.g., 1Cr–0.5Mo and 2.25Cr–1Mo) are widely used in high-temperature applications due to their creep ductility and resistance to oxidation and hydrogen embrittlement. Typical applications include turbine rotors and steam pipes, while power generation systems generally operate at around 823 K and ~50 Mpa (Evans 2023). Chromium–molybdenum steels are commonly classified into several groups, including 0.5Mo, 1Cr–0.5Mo, 2.25Cr–1Mo, higher chromium grades (5–9% Cr), and Cr–Mo–V steels, as well as modified Cr–Mo alloys (Davis (Ed.),1998, Gündoğdu 2012, Akgül 2011, Doğan 2014, Yangaz 2019). Typical applications of these alloys include pressure vessels, boilers, turbine casings, and forged rotors, operating at temperatures of approximately 350–500 °C, where temperature effects play a critical role in material design. To maintain the required mechanical properties, microstructural stability at elevated temperatures is essential. Superior creep resistance is primarily associated with the presence of stable and uniformly distributed carbide precipitates such as M_2C, M_7C_3, $M_{23}C_6$, and M_6C. Therefore, understanding the microstructural evolution of ferritic heat-resistant steels under different heat treatment conditions is of significant importance (Wang et al. 2013), Within a decade of its introduction, the Argon Oxygen Decarburization (AOD) process became the dominant route for stainless steel production, accounting for over 75% of global output. Compared to VOD, AOD offers simpler operation and more efficient slag removal, enabling cost-effective production of a wide range of alloys, including nickel- and cobalt-based superalloys and low-carbon stainless steels (down to ~0.02 wt.% C)(Swinbourne et al. 2012). The AOD process is recognized for its high efficiency and cost-effectiveness in steelmaking, enabling reduced levels of carbon, sulphur, nitrogen, and oxygen. It also minimizes sulphide and silicate inclusions, thereby improving mechanical performance. Typical compositions achieved are ~0.02–0.03 wt.% C and ~0.003–0.010 wt.% S ("AOD Process in Steel Production," n.d.,2025), In this study, the effects of different melting and refining routes on the microstructure, inclusion characteristics, and mechanical properties of G17CrMo5-5 cast steel are systematically investigated.

MATERIALS AND METHODS

In this study, the effects of different melting and refining routes on the microstructural and mechanical behavior of G17CrMo5-5 (ASTM A217 WC6) cast steel were investigated. Two routes were employed: (i) induction melting followed by Fe–Si–Zr, Ca–Si, and Al deoxidation, and (ii) induction melting followed by AOD refining with Ca–Si and Al deoxidation. The chemical compositions are given in Table 1a and 1b.

DOI: https://doi.org/10.30546/19023.978-9952-610-87-1.2026.100.1144.
ISBN: 978-9952-610-87-1

Table 1a. Chemical composition of WC6 (induction casting) (wt.%)

C	Si	Mn	P	S
0.18	0.48	0.71	0.012	0.006
Cr	Mo	Ni	Al	V
1.21	0.49	0.05	0.024	0.012

Table 1b. Chemical composition of WC6 (induction and AOD casting) (wt.%)

C	Si	Mn	P	S
0.20	0.49	0.69	0.015	0.002
Cr	Mo	Ni	Al	V
1.25	0.57	0.05	0.032	0.010

Melting was carried out at 1630–1635 °C, with ladle temperatures of approximately 1606–1610 °C for both processing routes. Brick ladles containing 80–85 wt.% Al_2O_3 were used, and the charge consisted mainly of DKP scrap and feeder additions with minor alloying adjustments.

Deoxidation in the induction route was performed using 0.03% Al, 0.097% Fe–Si–Zr, and 0.097% Ca–Si, whereas in the AOD route, ~0.60% Al and ~0.04% Ca–Si were used. All specimens were subjected to identical heat treatment: austenitization at ~930 °C, polymer quenching (~15%), and tempering at 720 °C to promote carbide precipitation and stabilize the bainitic–ferritic microstructure. This ensured that differences in properties were primarily due to melting and refining routes. Figure 1 illustrates the Argon–Oxygen Decarburization (AOD) process, highlighting molten steel refining by controlled gas injection and the associated decarburization mechanisms.

DOI: https://doi.org/10.30546/19023.978-9952-610-87-1.2026.100.1144.
ISBN: 978-9952-610-87-1

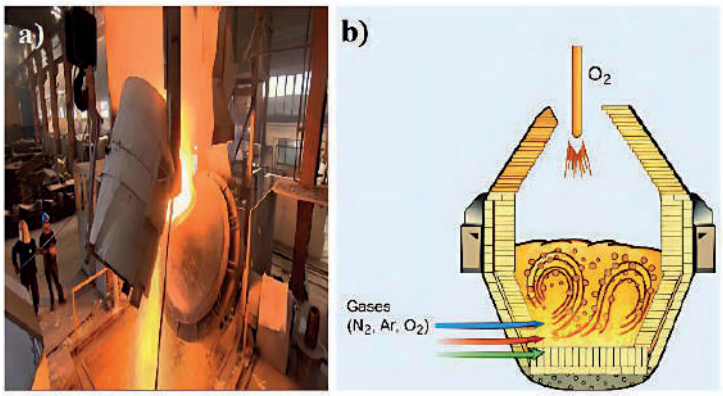

Figure 1. AOD process: (a) industrial view, (b) schematic with top oxygen blowing and bottom gas injection.

After casting and heat treatment, specimens were extracted from rectangular test blocks (70 × 70 × 250 mm). Standard metallographic preparation (sectioning, grinding, polishing, 4% Nital etching) was applied. Microstructural and inclusion analyses were performed using optical microscopy and SEM–EDS. Mechanical properties were evaluated by tensile, Charpy impact, and Brinell hardness tests (2.5 mm, 62.5 kg), and fracture surfaces were examined by SEM. The effects of processing routes on microstructure, inclusion evolution, and mechanical behavior were comparatively assessed.

RESULTS AND DISCUSSION

Figure 2 shows ground and polished images of samples produced by induction and induction followed by AOD. Residues are indicated by black arrows and discussed.

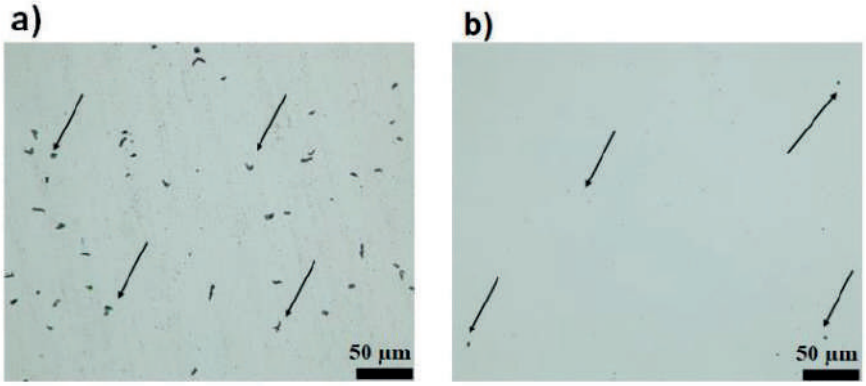

Figure 2. Polished images of samples

Optical micrographs (100×) show that inclusion density, morphology, and distribution in induction-cast samples strongly depend on refining practice. The induction condition is characterized by elongated,

DOI: https://doi.org/10.30546/19023.978-9952-610-87-1.2026.100.1144.
ISBN: 978-9952-610-87-1

preferentially oriented inclusions, consistent with Mn–S and Mn–Si–O residues reported in the literature (Chen et al.,2020). In contrast, AOD-processed samples exhibit finer and predominantly globular inclusions due to Ca–Si/Al deoxidation and argon stirring, promoting calcium-containing phases. This modification reduces stress concentrations and improves ductility and elongation (Higuchi et al.,1996), as further confirmed by SEM–EDS. The investigated Cr–Mo cast steels exhibit a ferrite–pearlite microstructure with uniformly distributed pearlite in a ferritic matrix. Thin, discontinuous grain-boundary carbides (likely $M_{23}C_6$) and fine intragranular MX-type precipitates are observed. Representative microstructures and phase identification are shown in Figure 3. The relatively low Cr and Mo contents stabilize the ferrite–pearlite equilibrium, governing phase distribution and precipitation behavior.

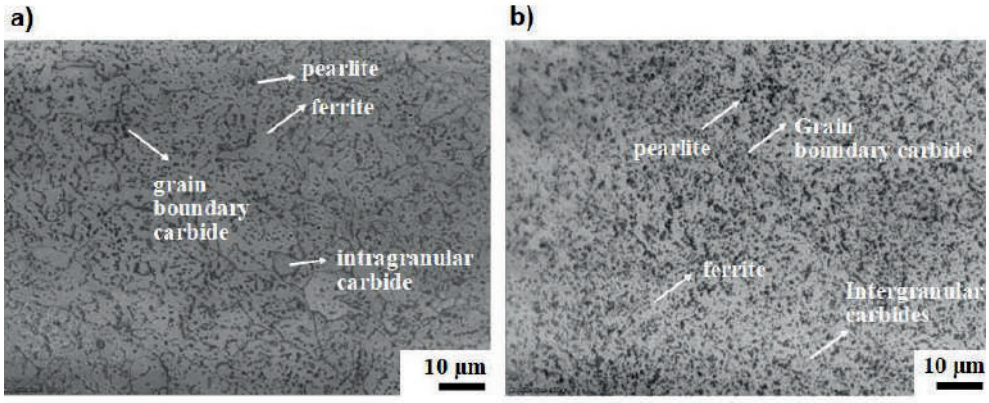

Figure 3. Optical microstructures of IND and IND+AOD.

In the induction-cast condition, pearlite colonies are well defined, with a relatively continuous grain-boundary carbide network. After AOD processing, Ca–Si/Al deoxidation and argon stirring promote oxygen removal, resulting in a thinner and more discontinuous carbide network and a more uniform, cleaner microstructure. This refinement reduces stress concentration and enhances elongation. SEM–EDS analysis revealed isolated, circular to semi-spherical inclusions with rough surfaces in the induction-cast material (Figure 4), exhibiting a multiphase layered structure composed of complex Fe–Al–Si–Mg–K–O oxides dominated by alumina-rich phases.

DOI: https://doi.org/10.30546/19023.978-9952-610-87-1.2026.100.1144.
ISBN: 978-9952-610-87-1

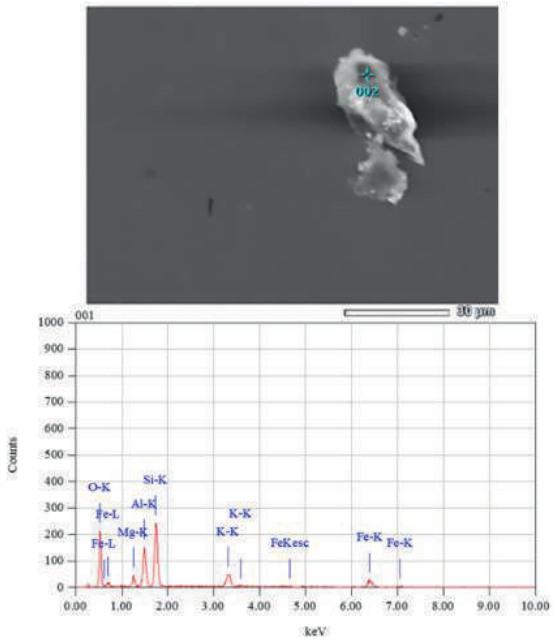

Figure 4.SEM–EDS images of sample induction casted

Mg and K are attributed to refractory-related contamination, while minor sulphur signals indicate limited oxysulfide formation, consistent with the low sulphur content (~0.006 wt.%). Overall, the inclusion characteristics reflect the combined effects of deoxidation and refractory–melt interactions.

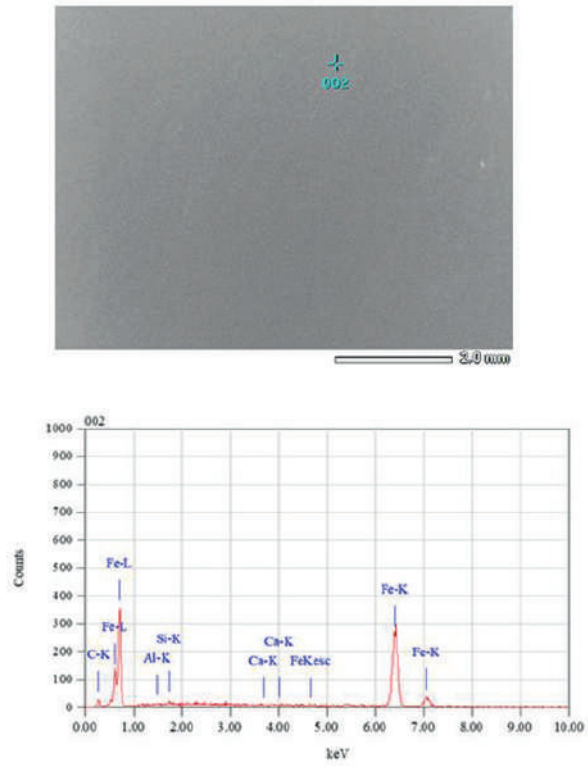

Figure 5. SEM–EDS characterization of inclusions after induction melting followed by AOD refining

DOI: https://doi.org/10.30546/19023.978-9952-610-87-1.2026.100.1144.
ISBN: 978-9952-610-87-1

SEM–EDS analysis of the induction + AOD processed G17CrMo5-5 alloy revealed small, uniformly distributed globular oxide inclusions (Figure 5). These were identified as Al–Si based oxides with dominant O and Si signals and low Al intensity, while only trace Ca and no Mn/MnS signals were detected, indicating effective sulphur removal. The refined inclusions result in a cleaner microstructure, reducing crack initiation and promoting ductile fracture, consistent with impact test results. Brinell hardness was measured using a 2.5 mm ball under a 62.5 kp load, with five indentations per sample averaged. The results (Table 2) were used to assess the influence of microstructure and inclusion density on hardness.

Table 2. Hardness Results (HB)

Sample	**1**	**2**	**3**	**4**	**5**	**Average**
IND+AOD	189	193	194	190	195	192.2
IND	174	176	175	177	176	175.6

The microstructure consists of a ferrite–pearlite matrix with thin, discontinuous grain-boundary carbides (likely $M_{23}C_6$). In the induction-cast condition, more continuous carbides and oriented Mn–Si–O/MnS inclusions increase heterogeneity. After AOD processing, a thinner carbide network and globular calcium aluminate inclusions produce a finer, more homogeneous matrix, accompanied by an increase in hardness from 175.6 to 192.2 HB. Room-temperature tensile and Charpy impact test results are summarized in Tables 3a and 3b. Tensile tests were performed according to EN ISO 6892-1, and impact tests according to ISO 148-1, with target values based on EN 10213.

Table 3a. Tensile test results at room temperature

Sample	Yield Strength (MPa)	Tensile Strength (MPa)	Elongation (%)	Reduction of Area (%)
Target	315	490-690	20	-
IND	462	620	18.6	63.53
IND+AOD	510	660	25	71.93

DOI: https://doi.org/10.30546/19023.978-9952-610-87-1.2026.100.1144.
ISBN: 978-9952-610-87-1

Table 3b. Charpy impact test results at room temperature

Sample	**Charpy Impact Energy (J at T_0)**		
	1	**2**	**3**
Target	**27 J**		
IND	58	54	70
IND+AOD	100	118	90

Tensile and Charpy results (Tables 3a–b) show that AOD processing improves mechanical performance, increasing strength (~460→510 MPa YS, ~620→660 MPa UTS), ductility (<20%→25%), and impact energy (~60→100 J). This enhancement is attributed to matrix refinement and globular inclusion formation, reducing crack initiation. Fracture surface analysis reveals a transition from mixed brittle–ductile features in the induction condition to predominantly ductile dimples after AOD, supporting the mechanical results. The induction-cast material exhibits a heterogeneous ferrite–pearlite microstructure with locally continuous grain-boundary carbides and Mn–Si–O/MnS inclusions, resulting in mixed fracture behavior with ductile dimples and localized brittle facets.

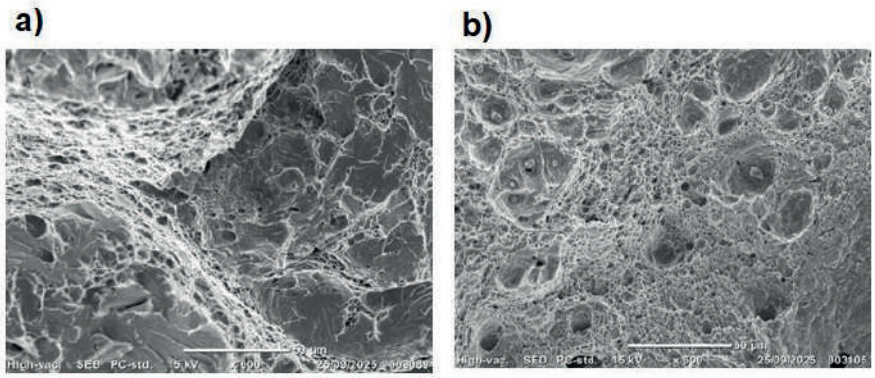

Figure 6. SEM images of fracture surfaces from Charpy impact tests at 600× magnification: a) induction and b) induction + AOD conditions.

Accordingly, Charpy impact energy is relatively low in the induction condition (~60 J). After AOD treatment, a cleaner and more homogeneous microstructure with spheroidized inclusions and a thinner carbide network is obtained, resulting in predominantly ductile fracture with fine dimples. This leads to a significant increase in impact energy to ~90–120 J (≈100 J).

DOI: https://doi.org/10.30546/19023.978-9952-610-87-1.2026.100.1144.
ISBN: 978-9952-610-87-1

CONCLUSION

This study demonstrates that AOD processing significantly improves the microstructural quality and mechanical performance of Cr–Mo cast steels. Compared to the induction condition, AOD promotes a cleaner, more homogeneous matrix through inclusion modification and carbide refinement, resulting in improved fracture behavior and a more balanced mechanical response. These results highlight the effectiveness of AOD as a robust metallurgical approach beyond simple chemical control.

• AOD processing significantly enhances microstructural cleanliness by modifying inclusion morphology and distribution.

• Induction casting is associated with heterogeneous matrix features, including oriented oxide–sulfide inclusions and locally continuous grain-boundary carbides.

• The AOD process transforms inclusions into fine, globular calcium aluminate phases and promotes carbide refinement.

• These microstructural changes suppress brittle fracture features and favor a predominantly ductile fracture mechanism.

• As a result, improved hardness, impact resistance, and a balanced strength–ductility response are achieved.

ACKNOWLEDGEMENTS

This study was conducted as part of the corresponding author's Ph.D. dissertation. The authors acknowledge Akmetal Metalurji Endüstrisi A.Ş. for providing experimental facilities and support. Laboratory and analytical services were provided by Hasçelik A.Ş., MacDermid Enthone Industrial Solutions, and Politeknik Metal Sanayi A.Ş. SEM–EDS analyses were conducted at Doğuş University.

REFERENCES

Aggen G, et al. 2005. ASM Handbook, Vol. 1: Properties and Selection: Irons, Steels, and High Performance Alloys. ASM International.

Akgül İ 2011. Investigation of the Corrosion Behavior of Cr–Mo Steel Used in the Petrochemical Industry. MSc Thesis, Karabük University, Türkiye.

Chaudhuri GRN 1990. Some Aspects of Mechanisms and Modelling of Creep Behaviour of 2.25Cr–1Mo Steel.

Chen C, et al. 2020. State of the art in the control of inclusions in spring steel for automobile applications. ISIJ International, 60: 617–627.

Davis JR (Ed.) 1998. Metals Handbook Desk Edition. 2nd ed. ASM International, CRC Press.

Doğan H 2014. Investigation of the Corrosion Properties of Low-Carbon Cr–Mo Steels with Different Grades. MSc Thesis, Karabük University, Türkiye.

Evans M 2023. Estimating threshold stresses using parametric equations for creep: Application to low-alloy steels. Materials Science and Technology, 39: 2302–2317.

Gündoğdu S 2012. Investigation of the Microstructural and Mechanical Properties of Welded Joints of Cr–Mo Steels. MSc Thesis, Karabük University, Türkiye.

Higuchi Y, et al. 1996. Inclusion modification by calcium treatment. ISIJ International, 36(Suppl.): S151–S154.

DOI: https://doi.org/10.30546/19023.978-9952-610-87-1.2026.100.1144.
ISBN: 978-9952-610-87-1

Studocu n.d. AOD Process in Steel Production: Principles and Advantages. Accessed 30 October 2025.

Swinbourne DR, et al. 2012. Understanding stainless steelmaking through computational thermodynamics: Part 3 – AOD converting. Transactions of the Institution of Mining and Metallurgy, Section C, 121: 23–31.

Wang W, Zhao W, Qu J 2013. Effect of heat treatment on microstructure and mechanical properties of 2.25Cr–1Mo steel. Steel Research International, 84: 178–183.

Yangaz M 2019. Effect of Heat Treatment on the Post-Weld Microstructural and Mechanical Properties of Valve Steel Used Under High-Temperature Conditions. MSc Thesis, Sakarya University, Türkiye.